ChemComm

Engineering a cleavable disulfide bond into a natural product siderophore using precursor-directed biosynthesis

Journal:	*ChemComm*
Manuscript ID	CC-COM-06-2018-004981.R1
Article Type:	Communication

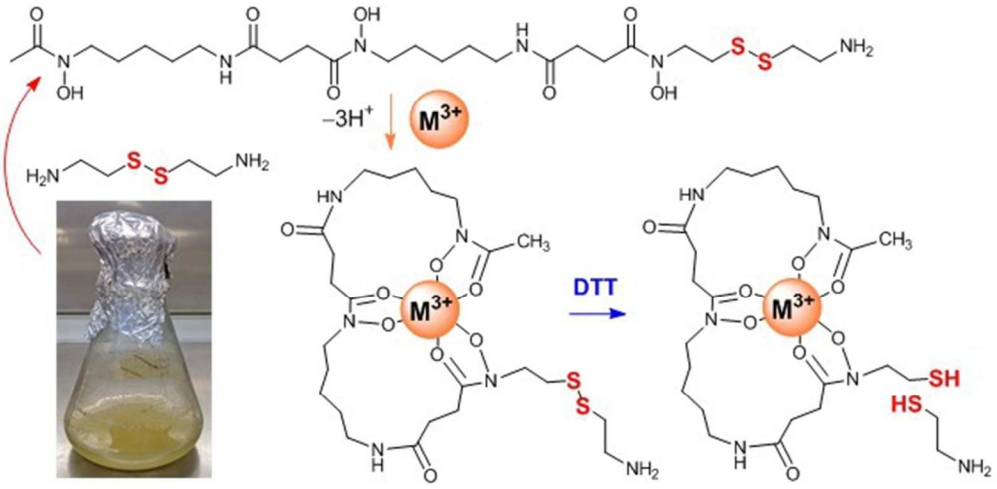

137x67mm (120 x 120 DPI)

Journal Name

COMMUNICATION

Engineering a cleavable disulfide bond into a natural product siderophore using precursor-directed biosynthesis

Received 00th January 20xx,
Accepted 00th January 20xx

DOI: 10.1039/x0xx00000x

www.rsc.org/

Tomas Richardson-Sanchez [a] and Rachel Codd*[a]

An analogue of the bacterial siderophore desferrioxamine B (DFOB) containing a disulfide motif in the backbone was produced from *Streptomyces pilosus* cultures supplemented with cystamine. Cystamine competed against native 1,5-diaminopentane during assembly. DFOB-$(SS)_1$[001] and its complexes with Fe(III) or Ga(III) were cleaved upon incubation with dithiothreitol. Compounds such as DFOB-$(SS)_1$[001] and its thiol-containing cleavage products could expand antibiotic strategies and Au-S-based nanotechnologies.

The small class of non-protein natural product metabolites that contain a disulfide motif display unique physicochemical and biological properties, with selected members (*eg*, romidepsin) showing clinical utility.[1] Methods to engineer S–S bonds into natural product metabolites could deliver analogues with broader applications in medicine and self-assembled monolayer (SAM)-based Au-S nanotechnologies, such as bio-sensing and bio-surveillance. Precursor-directed biosynthesis (PDB), whereby a producing organism is cultured in medium supplemented with non-native substrates, could have potential in this endeavour. This approach would require knowledge of the biosynthetic pathway of the target metabolite, and access to appropriate S–S-containing substrates.

Here, we demonstrate the use of PDB to engineer a disulfide motif into the backbone of the bacterial siderophore desferrioxamine B (**1**). The simplicity of the PDB approach makes it an attractive means to generate unusual analogues of structurally complex natural products, including siderophores.[2] Siderophores are low-molecular-weight organic compounds secreted by bacteria to acquire essential Fe(III) for growth.[3] The Fe(III)-siderophore complex is recognised by receptors at the cell surface of the source bacterium.[4] The selectivity of recognition provides a platform to develop siderophore-based antibiotic strategies.[5] The soil bacterium *Streptomyces pilosus* produces **1** as its native siderophore,[6] and is one of three agents used clinically to reduce excess Fe(III) that accumulates in patients with transfusion-dependent blood disorders.[7]

The biosynthesis of **1** is directed by the enzyme cluster DesABCD, with the first step involving the decarboxylation of L-lysine (DesA) to produce 1,5-diaminopentane (DP) as the major diamine substrate. Mono-*N*-hydroxylation of DP (DesB) produces *N*-hydroxy-DP (HDP), which is subject to *N*-acetylation (DesC) or *N*-succinylation (DesC) to give *N*-acetyl-*N*-hydroxy-DP (AHDP) or *N*-succinyl-*N*-hydroxy-DP (SHDP), respectively.[8] One unit of SHDP is then activated and condensed with AHDP (DesD, round 1) to form AHDP-SHDP. Activation and condensation of a second unit of SHDP to AHDP-SHDP (DesD, round 2) produces AHDP-SHDP-SHDP (**1**) (Fig. 1a).[9]

PDB has been used in recent work to produce analogues of **1** in *S. pilosus* cultures supplemented with non-native diamines that compete against DP. Viable non-native substrates include 1,4-diamino-2(*E*)-butene[9] and oxybis(ethanamine).[10] Here, we were interested in exploring the capacity of DesBCD to process substrates that were more structurally deviant from DP than this group. We selected cystamine (CS) (disulfanebis (ethanamine)), which compared to DP, is bent (C–S–S–C dihedral angle 100.1°), has a larger molecular volume (149 Å^3 vs 128 Å^3) and a greater dipole moment (2.83 D vs 1.57 D) (Fig. 2). Viability of CS as a substrate would produce a group of disulfide-containing analogues of **1** containing one (**2**–**4**), two (**5**–**7**) or a complete (**8**) DP-for-CS substrate exchange (Fig. 1b,c). Constitutional isomers within **2**–**4** or **5**–**7** arise from the insert position of CS, with the binary naming system (0, native; 1, non-native), as defined previously.[9] Additional merit of CS as a substrate was its potential to introduce cleavable disulfide bonds into a natural product siderophore. This could present new applications of siderophores as prodrugs, with constructs containing variably positioned disulfide motifs in the siderophore scaffold having potential to deliver conjugated antibiotics and/or toxic metal ions upon exposure to reducing conditions.

[a] *The University of Sydney, School of Medical Sciences (Pharmacology) and Bosch Institute, Camperdown New South Wales 2006, Australia. Rachel Codd: rachel.codd@sydney.edu.au*

Electronic Supplementary Information (ESI) available: [HRMS (**2**); MS isotope patterns (**1**, **2**, **9**, Fe(III) or Ga(III) complexes)]. See DOI: 10.1039/x0xx00000x

Cultures of *S. pilosus* were grown in base medium (control culture) or in medium supplemented with CS (10 mM).‡[11] The production of Fe(III)-coordinating species was monitored over 10 d by the absorbance value (500 nm) of an aliquot of supernatant with added Fe(III) (Fig. 2a).‡[12] The similarity between the data for the control and CS-supplemented cultures indicated that CS at 10 mM was not attenuating the production of Fe(III)-responsive compounds. At 10 d after inoculation, the cultures were harvested by centrifugation and the supernatant purified by XAD and IMAC chromatography and desalted for analysis by liquid chromatography-mass spectrometry (LC-MS).

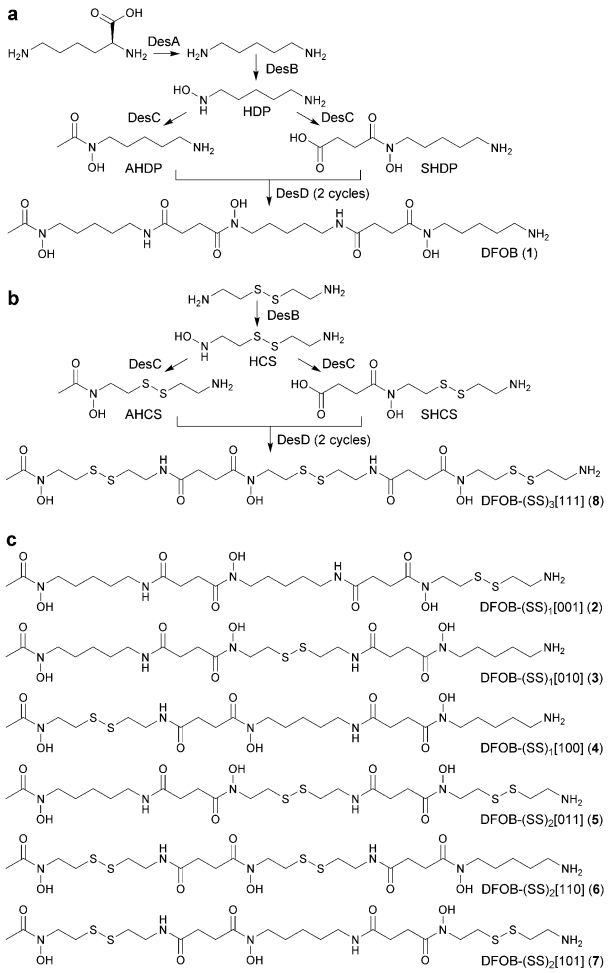

Fig. 1 Biosynthesis of (**a**) DFOB (**1**), (**b**) the disulfide analogue of DFOB from complete DP-for-CS substrate exchange (**8**), or (**c**) disulfide analogues of DFOB from partial DP-for-CS substrate exchange (**2**–**7**).

The LC-MS trace from the control culture (Fig. 2b, black) showed a major peak at 43.4 min, which corresponded with **1**. This peak from total ion current (TIC) detection was co-incident with a peak using the extracted ion chromatogram (EIC) mode set to the $[M+H]^+$ adduct of **1** (Fig. 2c). The LC-MS trace from the CS-supplemented culture showed **1** as the major species (Fig. 2b,c, grey), with an additional low-intensity peak present in the TIC at 46.6 min. The LC-MS traces in the CS-supplemented system with EIC values set to the $[M+H]^+$ adducts of **2**–**4**, **5**–**7** or **8** gave a peak at 46.7 min at EIC 611 (Fig. 2d, grey). This peak was not observed in the control culture (Fig. 2d, black) and was provisionally attributed to an analogue of **1** from the subset **2**–**4** containing one DP-for-CS substrate exchange. No peaks were detected that corresponded with **5**–**7** (Fig. 2e) or **8** (Fig. 2f).

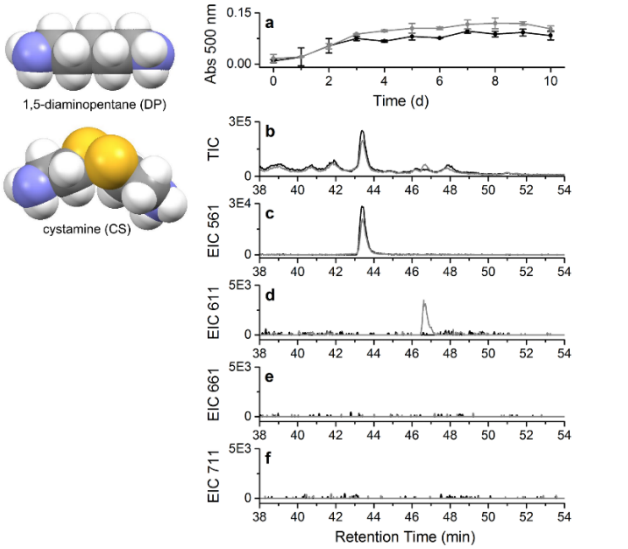

Fig. 2 Space-filling models of DP and CS. (**a**) Visible absorption (λ 500 nm) from aliquots of *S. pilosus* supernatant (0–10 d) analysed with added Fe(III), from control (black) or CS-supplemented cultures (grey). LC-MS traces from semi-purified *S. pilosus* supernatant (10 d) from control (black) or CS-supplemented cultures (grey), detected as (**b**) TIC, or EIC with values corresponding with the $[M+H]^+$ adducts of (**c**) **1**, (**d**) **2**–**4**, (**e**) **5**–**7**, or (**f**) **8**.

LC-MS/MS analysis was undertaken on the CS-supplemented sample (Fig. 3). The peak identified as **1** using selected ion monitoring (SIM) was subject to fragmentation, with the data in agreement with the predicted fragmentation pattern for **1** (Fig. 3a-c).[9-10] Analogous processing of the peak assigned to **2**–**4** gave a MS fragmentation pattern that matched the predicted pattern of **2** (Fig. 3d-f), in which the CS-derived substrate was inserted at the amine-containing region of **1**. Fragments observed at *m/z* 169.0, 251.1, 369.2 and 451.2 were not present in the pattern for **1** and were consistent with an analogue of **1** with one DP-for-CS substrate exchange. Fragments at *m/z* 169.0, 361.2 and 443.3 confirmed the isomer as **2**, since among **2**–**4**, these fragments are unique to **2**. There was no evidence of **3**–**4**, based on the absence of characteristic fragments at *m/z* 119.1 (**3**,**4**), 194.1 (**4**), 319.2 (**4**), 411.2 (**3**,**4**) or 493.3 (**3**,**4**). The peak containing **2** was collected by semi-preparative HPLC, with HRMS analysis (found $[M+H]^+$ 611.28927, $[C_{24}H_{47}N_6O_8S_2]^+$ requires 611.28913) consistent with **2** (Fig. S1, ESI†). The yield of **2** was approximately 0.5 mg per 50 mL culture. Based on the relative peak areas (88%:12%) of **1** (100% DP) and **2** (66.6% DP, 33.3% CS), the rate of CS incorporation was 4%. This was similar to the incorporation of 1,6-diaminohexane in macrocyclic desferrioxamine E.[2a] The integrity of **2** as a siderophore was shown by MS measurements from solutions of Fe(III) and **2**, which gave MS isotope patterns consistent with the $[M+2H]^{2+}$, $[M+H]^+$ and $[M+Na]^+$ (where M is [Fe(III)-**2**(3−)]) (Fig. S2, ESI†).

The biosynthesis of **2** demonstrates that CS is a viable substrate for DesB to form *N*-hydroxy-CS (HCS) and that HCS remains a viable substrate for DesC-mediated *N*-succinylation to form *N*-succinyl-N-hydroxy-CS (SHCS). The final product **2**

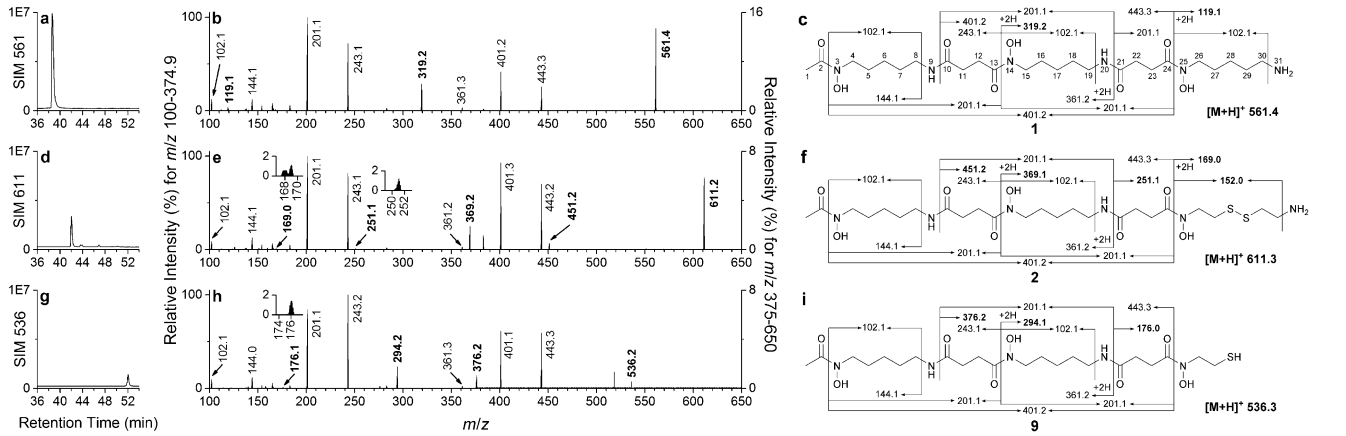

Fig 3 LC-MS trace (left) and experimental (middle) or predicted (right) MS/MS fragmentation of **1** (**a**–**c**), **2** (**d**–**f**) or **9** (**g**–**i**). Fragments unique to **1**, **2** or **9** are in bold (middle, right).

would be formed following the second cycle of DesD catalysed condensation of SHCS with AHDP-SHDP, which is the native dimer precursor of **1**[9] and common to **2**.The absence of **3** and **4** could be attributed to one or a combination of the following steps being unviable: (i) *N*-acetylation of HCS (DesC); first round condensation (DesD) of (ii) SHCS with AHDP (dimer precursor of **3**); and/or (iii) SHDP with AHCS (dimer precursor of **4**); second round condensation (DesD) of SHDP with (iv) AHDP-SHCS to form **3**; and/or (v) AHCS-SHDP to form **4**. While the AHDP-SHDP dimer precursor common to **1** and **2** was detected (*m/z* 361.2), no peaks were detected that corresponded with AHDP-SHCS, AHCS-SHDP or AHCS-SHCS, which suggests that the biosynthetic pathway for **3** and **4**, and for **5**–**8**, is more likely halted at upstream steps (i)–(iii) than downstream steps (iv)–(v).

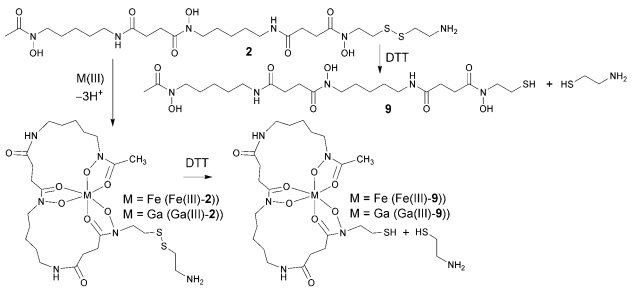

Fig. 4 Coordination between **2** and Fe(III) or Ga(III) to form Fe(III)-**2** or Ga(III)-**2**, respectively. Cleavage of the disulfide bond in **2**, Fe(III)-**2** or Ga(III)-**2** with dithiothreitol (DTT) to form 2-aminoethanethiol and **9**, Fe(III)-**9** or Ga(III)-**9**, respectively.

Cleavage of the disulfide bond of **2** was predicted to release 2-aminoethanethiol and **9** (Fig. 4). The potential to use **2** with an antibiotic covalently bound at the amine terminus as a prodrug for antibiotic delivery could require S–S bond cleavage of Fe(III)-**2** or Ga(III)-**2**, assuming that bacterial cell-surface recognition of **1** is optimised for the metal-siderophore complex rather than the free ligand.[4] Aliquots of the semi-purified supernatant from the control and CS-supplemented cultures, in the absence or presence of Fe(III) or Ga(III), were incubated with dithiothreitol (DTT) at a final concentration of 2 or 10 mM. LC-MS analysis used SIM detection, with values set for species relevant to each system (Fig. 5).

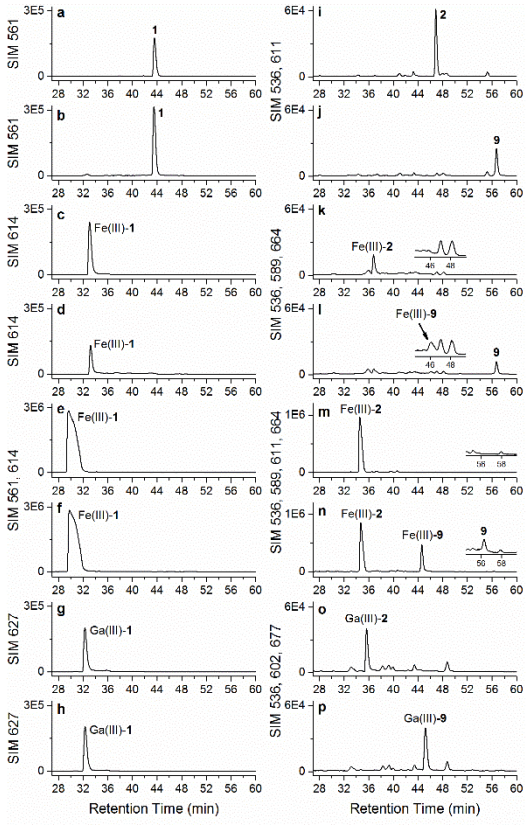

Fig 5 LC-MS traces from semi-purified *S. pilosus* supernatant from control (**a**–**h**) or CS-supplemented (**i**–**p**) cultures, in the absence (**a**, **b**, **i**, **j**) or presence of Fe(III) (**c**–**f**, **k**–**n**) or Ga(III) (**g**, **h**, **o**, **p**); and in the absence (**a**, **c**, **e**, **g**, **i**, **k**, **m**, **o**) or presence of DTT at 10 mM (**b**, **d**, **h**, **j**, **l**, **p**) or 2 mM (**f**, **n**). SIM values (single or multiple) corresponded with **1** (561), **2** (611), **9** (536), Fe(III)-**1** (614), Ga(III)-**1** (627), Fe(III)-**2** (664), Ga(III)-**2** (677), Fe(III)-**9** (589), Ga(III)-**9** (602). Selected data (**e**, **f**, **m**, **n**) were acquired at a later day, giving different retention times for a given species, due to instrumental variability.

The LC-MS trace from the control culture in the absence (Fig. 5a) or presence of 10 mM DTT (Fig. 5b) gave a peak for **1** (Fig. 5b). The peak for **2** in the CS-supplemented culture (Fig. 5i) disappeared in the presence of 10 mM DTT, with a new peak appearing at 56.7 min that, based on the SIM detection, was provisionally assigned to **9** (Fig. 5j). Confirmation was provided

from LC-MS/MS analysis, with fragments at *m/z* 176.1, 294.2 and 376.2 characteristic of the predicted pattern for **9** (Fig. 3g-i). This demonstrated the veracity of reductive S–S bond cleavage of **2** to give **9**. The intensity of the signal for Fe(III)-**1** in the control culture was attenuated with 10 mM DTT (Fig. 5c,d).[13] The signal for Fe(III)-**2** in the CS-supplemented culture was diminished upon incubation with 10 mM DTT, with the appearance of a low-intensity signal for Fe(III)-**9** and a signal in a higher relative intensity for **9** (Fig. 5k,l). Subsequent analysis of a second Fe(III)-**2**-containing sample treated with DTT at a lower concentration (2 mM) showed the presence of unreacted Fe(III)-**2**, together with Fe(III)-**9**, and a low-intensity signal for **9** (Fig. 5m,n). Redox-inactive Ga(III), which forms high-affinity complexes with siderophores,[14] was examined as a substitute for Fe(III). The signal for Ga(III)-**1** in the control culture showed minimal diminution in the presence of DTT at 10 mM (Fig. 5g,h). In the case of Ga(III)-**2** in the pre-DTT treated CS-supplemented sample, incubation with DTT gave a well resolved signal for Ga(III)-**9** with no discernible signal for **9** (Fig. 5o,p). This supported the DTT-mediated reduction of the S–S bond in redox-inactive Ga(III)-**2** gave Ga(III)-**9** as the major product, with no evidence of complex dissociation. Experimental MS isotope patterns for all species agreed with calculated data (Fig. S2, ESI†).

In conclusion, a cleavable disulfide bond has been engineered into the amine-containing region of the bacterial siderophore **1** to produce **2**. The PDB production method involved culturing the native **1**-producer *S. pilosus* in CS-supplemented medium and is attractive in its simplicity. The veracity of DTT-mediated S–S bond cleavage of **2** to produce thiol **9** was demonstrated. DTT-mediated cleavage of the S–S bond in Ga(III)-**2** produced Ga(III)-**9** in an apparent 1:1 stoichiometric conversion, with lower conversion of Fe(III)-**2** to Fe(III)-**9**, likely due to Fe(III)/(II) redox chemistry. Covalent attachment of an antibiotic to the amine terminus of **2** could have potential as an antibiotic prodrug recognised as the Ga(III)- or Fe(III)-complex by pathogenic bacteria, such as *Staphylococcus aureus* or *Vibrio furnissi*,[15] that use **1** as a xenosiderophore. Cell-surface uptake of the Fe(III)-**2**- or Ga(III)-**2**-antibiotic conjugate could be followed by antibiotic release upon exposure to intracellular reductants. Work published during the period that the current study was under review supports this strategy.[16] Disulfide- and thiol-containing analogues of native bacterial siderophores, such as **2** and **9**, respectively, could have applications in bio-sensing and bio-surveillance and other Au–S-dependent self-assembled monolayer (SAM) nano-technologies or nano-medicines.[17]

This work was supported by the Australian Research Council (DP180100785 to RC) and The University of Sydney (Australian Postgraduate Award to TRS).

Conflicts of interest

There are no conflicts to declare.

Notes and references

1 (*a*) A. J. Waldman, T. L. Ng, P. Wang and E. P. Balskus, *Chem. Rev.*, 2017, **117**, 5784-5863; (*b*) J. Li, C. Wang, Z.-M. Zhang, Y.-Q. Cheng and J. Zhou, *Sci. Rep.*, 2014, **4**, 4145.

2 (*a*) J. Meiwes, H.-P. Fiedler, H. Zähner, S. Konetschny-Rapp and G. Jung, *Appl. Microbiol. Biotechnol.*, 1990, **32**, 505-510; (*b*) S. Konetschny-Rapp, G. Jung, K. N. Raymond, J. Meiwes and H. Zaehner, *J. Am. Chem. Soc.*, 1992, **114**, 2224-2230; (*c*) G. J. Feistner, D. C. Stahl and A. H. Gabrik, *Org. Mass Spectrom.*, 1993, **28**, 163-175; (*d*) C. Z. Soe and R. Codd, *ACS Chem. Biol.*, 2014, **9**, 945-956.

3 (*a*) K. N. Raymond and E. A. Dertz, in *Iron Transport in Bacteria*, eds. J. H. Crosa, A. R. Mey and S. M. Payne, ASM Press, Washington, DC, 2004, pp. 3-17; (*b*) R. C. Hider and X. Kong, *Nat. Prod. Rep.*, 2010, **27**, 637-657.

4 (*a*) J. H. Crosa, A. R. Mey and S. M. Payne, *Iron transport in bacteria*, ASM Press, Washington, 2004; (*b*) M. Miethke and M. A. Marahiel, *Microbiol. Mol. Biol. Rev.*, 2007, **71**, 413-451.

5 (*a*) C. Hennard, Q. C. Truong, J.-F. Desnottes, J.-M. Paris, N. J. Moreau and M. A. Abdallah, *J. Med. Chem.*, 2001, **44**, 2139-2151; (*b*) F. Rivault, C. Liebert, A. Burger, F. Hoegy, M. A. Abdallah, I. J. Schalk and G. L. A. Mislin, *Bioorg. Med. Chem. Lett.*, 2007, **17**, 640-644; (*c*) U. Möllmann, L. Heinisch, A. Bauernfeind, T. Köhler and D. Ankel-Fuchs, *BioMetals*, 2009, **22**, 615-624; (*d*) C. Ji, R. E. Juárez-Hernández and M. J. Miller, *Future Med. Chem.*, 2012, **4**, 297-313; (*e*) T. A. Wencewicz and M. J. Miller, *J. Med. Chem.*, 2013, **56**, 4044-4052; (*f*) T. A. Wencewicz and M. J. Miller, *Top. Med. Chem.*, 2017, **26**, 151-184; (*g*) R. Liu, P. A. Miller, S. B. Vakulenko, N. K. Stewart, W. C. Boggess and M. J. Miller, *J. Med. Chem.*, 2018, **61**, 3845-3854; (*h*) W. Neumann, M. Sassone-Corsi, M. Raffatellu and E. M. Nolan, *J. Am. Chem. Soc.*, 2018, **140**, 5193-5201.

6 R. Codd, T. Richardson-Sanchez, T. J. Telfer and M. P. Gotsbacher, *ACS Chem. Biol.*, 2018, **13**, 11-25.

7 P. V. Bernhardt, *Dalton Trans.*, 2007, 3214-3220.

8 (*a*) F. Barona-Gómez, U. Wong, A. E. Giannakopulos, P. J. Derrick and G. L. Challis, *J. Am. Chem. Soc.*, 2004, **126**, 16282-16283; (*b*) G. L. Challis, *ChemBioChem*, 2005, **6**, 601-611; (*c*) N. Kadi, D. Oves-Costales, F. Barona-Gómez and G. L. Challis, *Nat. Chem. Biol.*, 2007, **3**, 652-656.

9 T. J. Telfer, M. P. Gotsbacher, C. Z. Soe and R. Codd, *ACS Chem. Biol.*, 2016, **11**, 1452-1462.

10 T. Richardson-Sanchez, W. Tieu, M. P. Gotsbacher, T. J. Telfer and R. Codd, *Org. Biomol. Chem.*, 2017, **15**, 5719-5730.

11 At 40 mM CS, no Fe(III)-coordinating species were detected, including **1**. Cell growth was slower and less dense. Although **2** was observed at 20 mM CS in yields about twice observed at 10 mM, the lower concentration was selected to maintain a conservative approach towards production versus potential toxicity.

12 The non-homogeneous growth of *S. pilosus* in liquid medium prevents the use of conventional OD measurements of cell growth. This Fe(III)-addition assay is a surrogate measure of culture progress.

13 This could be due to Fe(III)/Fe(II) reduction and the formation of neutral, MS-silent Fe(II)-**1** (in positive-ion mode), and/or the dissociation of Fe(II)-**1** to give **1** and/or **1**-adducts. **1** was not detected (EIC (**d**), SIM (**f**)), which suggested that any **1** that may have been liberated from the dissociation of Fe(II)-**1** was subject to further Fe(III)/(II)/DTT-mediated chemistry.

14 A. Evers, R. D. Hancock, A. E. Martell and R. J. Motekaitis, *Inorg. Chem.*, 1989, **28**, 2189-2195.

15 (*a*) N. P. Endicott, E. Lee and T. A. Wencewicz, *ACS Infect. Dis.*, 2017, **3**, 542-553; (*b*) T. Tanabe, T. Funahashi, K. Miyamoto, H. Tsujibo and Y. S., *Biol. Pharm. Bull.*, 2011, **34**, 570-574.

16 W. Neumann and E. M. Nolan, *J. Biol. Inorg. Chem.*, 2018, doi: 10.1007/s00775-018-1588-y.

17 (*a*) C. Vericat, M. E. Vela, G. Benitez, P. Carro and R. C. Salvarezza, *Chem. Soc. Rev.*, 2010, **39**, 1805-1834; (*b*) Y. Wang, D. Liu, Q. Zheng, Q. Zhao, H. Zhang, Y. Ma, J. K. Fallon, Q. Fu, M. T. Haynes, G. Lin, R. Zhang, D. Wang, X. Yang, L. Zhao, Z. He and F. Liu, *Nano Lett.*, 2014, **14**, 5577-5583.